Proceedings of ICFDP9:
Ninth International Congress of Fluid Dynamics & Propulsion
December 18-21, 2008, Alexandria, Egypt

ICFDP9-EG-212

Study of the Influence of Orifice Flow meter on the Characteristics of Oil-in-Water Emulsion Flow Using Image Processing

Mohamed F. Khalil
Department of Mechanical Engineering,
Faculty of Engineering, Alexandria University,
Alexandria 21544, Egypt
mfaridkhalil@yahoo.com

Sadek Z. Kassab
Department of Mechanical Engineering,
Faculty of Engineering, Alexandria University,
Alexandria 21544, Egypt
szkassab@yahoo.com

Ashraf S. Ismail
Department of Engineering Mathematics and Physics,
Faculty of Engineering, Alexandria University,
Alexandria 21544, Egypt
ashraf_s_ismail@yahoo.com

Ibrahim S. Elazab
Department of Mechanical Engineering,
Faculty of Engineering, Alexandria University,
Alexandria 21544, Egypt
shoshaibrahimsaad@yahoo.com

ABSTRACT

A photographic and subsequent image analysis technique was used to determine upstream and downstream droplet size distribution in unstable oil-in-water emulsion flowing through orifice restrictor, at different holdup and Reynolds number. The images were automatically treated, analyzed and several object descriptors obtained for each droplet using Matlab software. Orifice coefficient of discharge was calculated from the measurements of orifice head difference and flow rate at different values of holdup for stable and unstable oil-in-water emulsion flow. Empirical relations are derived to describe the orifice coefficient of discharge. The coefficient of discharge decreases and orifice head difference increases as the holdup increase. For stable o/w emulsion, the type of emulsifier has pronounced effect on coefficient of discharge and orifice head difference. The unstable o/w emulsion has greater value of coefficient of discharge and smaller orifice head difference compared with stable emulsion.

The upstream and downstream mean droplet diameter, calculated from the droplet size distribution resulting from image analysis, at different velocities is presented. The downstream mean droplet diameter is smaller than the upstream one, due to breakup of drops passing through the orifice. The droplet breakup increases as the emulsion velocity increase. As the holdup increased the mean droplet diameter increases, and this attributed to the droplet coalescence process.

KEYWORDS:

Orifice flow, Droplet size distribution, Emulsion, Droplet break-up, Image processing.

INTRODUCTION

In the petroleum recovery industry, oil extraction is often accompanied with a high water throughput. Depending on the flow geometry, mixture velocity and phase ratio, the two-liquid phase flow may be dispersed, stratified or mixed. In all cases, the occurrence of cross-sectional restrictions along the pipe will enhance the dispersing process by increasing the fragmentation rate of liquid-liquid interfaces Galinat et al.[1].

Understanding and modeling the breakup process induced by a pipe restriction in liquid-liquid dispersion is an important issue in view of a better prediction of the droplet size distribution and improving the scale-up and design of oil-water separators.

Buhidma, and Pal, [2] studied the behavior of oil-in-water emulsion through a wedge meters and segmental orifice meters of various shapes and sizes. They found that a wedge meters and segmental orifice meters are feasible flowmetering devices for two phase oil-water emulsions and also the discharge coefficient is constant over a wide range of Reynolds number.

Mayor, et al.[3] using an image analysis technique for the study of continuous co current gas-liquid slug flow, in vertical columns, The technique allows the straightforward measurement of several slug flow characteristics with almost no input from the operator, also the evaluation of the uncertainty associated with the parameters measured with the proposed technique is preformed.

Percy and Sleicher [4] obtained experimental data to demonstrate the effect of concentric orifices on droplet breakup of liquid-liquid systems at low holdup flowing through the orifices. The drop fragments drifted upward against the pipe wall and were measured in the longitudinal direction. The number of drop originally present and the percent breakup were calculated from the total volume of the fragments and the initial drop diameter. The relations for orifice size (β) required for effectively complete breakup were introduced.

On the other hand, in past decade optical measurement techniques have received wide attention in the scientific community. Electrical capacitance tomography has been under rapid development, and it seems better suited for coherent pipe flows. In comparison to other measurement techniques, image analysis is non-destructive and is characterized by a great speed, which is very important in on-line systems. Berthiaux et al.[5] applied image analysis to two free-flow powders differing in colour mixed by a continuous static mixing unit and poured for transport by a belt conveyor without disturbance. A charge-coupled device (CCD) camera placed on the conveying line captures images of the moving belt. These images are then treated with specially designed computer software to calculate the homogeneity ratio of the mixture.

Meijer et al.[6] developed a fast light microscope method to evaluate cosmetic emulsion droplet size and dispersion, in which a light microscope instrument was utilized, and a standard sample pretreatment procedure and microscope image acquisition method were optimized. A BX 60 light microscope with bright field illumination module and 3 (CCD) camera was utilized in the study. Twenty-four-bit images (RGB, red, green, blue) were used with fixed settings of illumination, contrast, brightness, scale, and threshold to ensure consistency. Then, the image is acquired and spatial calibration is performed to establish a size relationship for objects in the image frame. A special macro program was created to perform the data treatment steps automatically. .

Lovick et al. [7] used a light back scattering technique (3 Dimensional Optical Reflectance Measurement technique, 3D ORM) to obtain on-line drop size distributions in unstable kerosene-in-water dispersions for dispersed phase fractions from 10% to 60%. The results from the 3D ORM technique were compared with those in-situ video recording obtained with an endoscope attached to a high-speed camera.

Several methods exist for measuring the interfacial area in gas-liquid systems, such as photographic, light attenuation, ultrasonic attenuation, double-optical probes and chemical absorption methods. But these methods are effective only under specific conditions. Mena et al. [8], used photographic and a subsequent image analysis technique to determine bubble characteristics, such as superficial area, size and shape, in air-water-calcium alginate beads system in bubble column.

Khalil et al. [9, 10] performed an indepth Study Using Image Processing for the Friction Losses Accompanied the Flow of Oil-in-Water Emulsions through Pipes and pipe fitting.

In the present study, photographic and subsequent image analysis technique was used to determine upstream and downstream droplet size distribution in unstable oil-in-water emulsion flowing through orifice restrictor, at different holdup and velocities. In addition orifice meter coefficient of discharge have been calculated from the measurements of orifice head difference and flow rate at different values of holdup for stable and unstable oil-in-water emulsion flow. Empirical relations are derived to describe the orifice coefficient of discharge.

EXPERIMENTAL SETUP AND PROCEDURE

APPARATUS

Figure (1) shows the test rig that is designed to investigate the o/w emulsion flow through orifice of diameter 10 mm, fixed in 25mm PVC Pipe. The emulsions is prepared in a large tank (1 m^3 capacity) equipped with two high shear mixers, electric heater with temperature controller. The emulsion from the preparation tank is circulated to the pipeline test sections by a centrifugal pump. The flow rate is measured by orifice meter and controlled by gate valve after the pump. The pressure drop across the orifice is measured by manometers.

EMULSION PREPARATION

Emulsion preparation was given in details by Khalil et al.[9-11] and it is repeated here for the sake of completeness and self content. Three different sets of emulsions were prepared using tap water and a refined white mineral oil. In one set, no chemical-emulsifier (surfactant) added so that unstable emulsion is produced. The unstable emulsion separated into oil and water if left without agitation for sometime. In the second set , a surfactant namely Fatty Acid and Amine, FAA, which prepared as follows, 3% Oleic Acid [$C_{18}H_{34}O_2$] from the total volume of mineral oil, and 1% Trimethylamine [C_3H_9N] from the total volume of water. In the third set, an ionic surfactant namely Sodium Dodecyl Sulfate, SDS, [$CH_3\ (CH_2)_{11}\ OSO_3Na$] is added, to the oil with 1.5% by weight based on the water.

For the cases of image processing experiments the Methylene Blue dye [$C_{16}\ H_{18}\ Cl\ N_3\ S\ 3H_2O$] is used to color the water only and added with concentration 0.01 g/L (4.8 ppm). The image quality increased due to the difference between the colored water and oil. It is important to point out that the Methylene Blue dye has no effect on the properties of

water or oil and do not act as a surfactant [12, 13], it is used as indicator to give better results with the image processing [14].

IMAGE PROCESSING

To capture pictures for emulsion upstream and downstream the orifice, two glass tubes, of 15 cm length and 25 mm diameter, are fixed inserted and after the orifice. A panasonic lumix DMC-LZ1, 4 mega pixel camera with CCD sensor, shutter speed (1/2000) s, and 6x optical zoom is utilized in the study.

Preliminary experiments show that unclear image with small oil drops, in case of low holdup, and in case of high holdup oil drops coalescence phenomena inhibit clear image. Moreover the camera could not capture clear image for stable oil-in-water emulsion as surfactant makes mixture in an emulsification form. Consequently, in order to obtain clear image processing results, the present image processing study is restricted to unstable emulsion.

Photographic and a subsequent image analysis technique, Fig. (9), is utilized to determine drop size distribution upstream and downstream the orifice (β=0.4), in unstable oil-water emulsion at holdup 30%, 45%, and 55%. Images were grabbed with a digital camera. Sets of images (300 ppi) were captured for varying emulsion velocities and holdup. Then, the images were automatically treated, analyzed and several object descriptors obtained for each drop using Matlab 7.1 software.

Twenty-four-bit images (RGB, red, green, blue) were used with fixed settings of illumination, contrast, brightness, scale, and threshold to ensure consistency. Then, the image is acquired and spatial calibration is performed to establish a size relationship for objects in the image frame. A special program on Matlab software was created to perform the data treatment steps automatically. The steps involved:

1- Read in the 'unstable emulsion .jpg' image, which is a photograph of unstable oil-water emulsion flow through orifice meter, Fig. (9-1).
2- Convert RGB image to class of double (the most mathematical operation in Matlab software is only supported for data of class double), Fig. (9-2).
3- Convert RGB image (class double) to gray scale (it must be to convert the input image to gray scale format and then uses threshold to convert this gray scale image to binary image) Fig. (9-3).
4- Reduced noise by using median filter (3*3), Fig.(9-4).
5- To maximize the intensity contrast in the image. You can do this using the function 'Adapthisteq', which performs contrast-limited adaptive histogram equalization. Rescale the image intensity using the function 'Imadjust' so that it fills the data type's entire dynamic range, Fig.(9-5).
6 - Estimate the Value of Background Pixels.
The background illumination is brighter in the center of the image than at the bottom. In this step, the example uses a morphological opening operation to estimate the background illumination, Fig.(9-6).
7- Create an image with a uniform background, fig.(9-7)
8- Convert an image to a binary image.
Binary image containing only black and white pixels based on threshold (the point at which an action begins or change) where binary image is stored as logical array containing only 0's and 1's interpreted as a black and white respectively then the values of 1's collected which theses values represent the summation of oil drops area meanwhile the remaining from image pixels map represent water area.
The Methylene Blue dye is used to color the water and thus, increase the contrast between water and oil. This enhances the image process. The threshold is adjusted according to the holdup value, Fig.(9-8).
9. - Determine Surface Area Distribution in binary image.
Granulometry estimates the surface area distribution of oil drops as a function of size. Granulometry likens image objects to stones whose sizes can be determined by sifting them through screens of increasing size and collecting what remains after each pass. Image objects are sifted by opening the image with a structuring element of increasing size and counting the remaining surface area (summation of pixel values in the image) after each opening. Choose a counter limit so that the surface area goes to zero as you increase the size of the structuring element. For display purposes, leave the first entry in the surface area array empty, Fig.(9-11).
10 - Calculate First Derivative of Distribution.
A significant drop in surface area between two consecutive openings indicates that the image contains objects of comparable size to the smaller opening. This is equivalent to the first derivative of the surface area array, which contains the size distribution of the oil drops in the image. Calculate the first derivative with the DIFF function Fig. (9-12).
12 - Extract oil drops having a particular radius.
Notice the minima and the radii where they occur in the graph. The minima tell you that oil drops in the image have those radii. The more negative the minimum point, the higher the oil drops' cumulative intensity at that radius, Figs. (9-9 and 9-10).
From the pixels histogram and its differentiation, the droplet size distribution is obtained, and the mean droplet diameter is calculated as follows:

$$a_m = \frac{\sum_i N_i a_i}{\sum_i N_i} \qquad (1)$$

where a_m is the mean droplet area, and N_i is the number of droplets of area a_i.

IMAGE PROCESSING UNCERTAINTY

$$d_{,m} = d_{,px} \cdot \frac{h_{cal,m}}{h_{cal,px}}$$

(2)

Where:
$d_{,m}$ is the droplet diameter in meter and $d_{,px}$ is the droplet diameter in pixels. $h_{cal,m}$ and $h_{cal,px}$ refer to the height of the calibration element in meters and pixels units, respectively.

$$(\delta d_{,m})^2 = \left(\frac{\partial d_{,m}}{\partial d_{,px}}\delta d_{,px}\right)^2 + \left(\frac{\partial d_{,m}}{\partial h_{cal,m}}\delta h_{cal,m}\right)^2 + \left(\frac{\partial d_{,m}}{\partial h_{cal,px}}\delta h_{cal,px}\right)^2$$

(3)

$$(\delta d_{,m})^2 = \left(\frac{h_{cal,m}}{h_{cal,px}}\delta d_{,px}\right)^2 + \left(\frac{d_{,px}}{h_{cal,px}}\delta h_{cal,m}\right)^2 + \left(\frac{-h_{cal,m}.d_{,px}}{(h_{cal,px})^2}\delta h_{cal,px}\right)^2$$

(4)

$$\frac{\delta d,m}{d,m} = \sqrt{\left(\frac{h_{cal},m}{h_{cal},pxd,m}\delta d,px\right)^2 + \left(\frac{d,px}{h_{cal},pxd,m}\delta h_{cal},m\right)^2 + \left(\frac{h_{cal},md,px}{(h_{cal},px)^2 d,m}\delta h_{cal},px\right)^2}$$

(5)

Where $\delta d_{,m}$ is the uncertainty of the droplet diameter. The values of parameters and absolute uncertainties in the calculation are shown in table (1)

Table 1
Values of parameters and absolute uncertainty in the calculation of droplet uncertainty

Parameter	units	value
$\delta d,px$	Pixel	1
h_{cal},m	[m]	10^{-4}
h_{cal},px	Pixel	28.95
$\delta h_{cal},m$	[m]	10^{-5}
$\delta h_{cal},px$	Pixel	1

The relation uncertainties in droplet diameters $\left(\frac{\delta d,m}{d,m}\right)$ are shown in table (2).

Table (2) The relation uncertainties in droplet diameters.

d,px	d,m	$\left(\frac{\delta d,m}{d,m}\right)$
1	0.000055	0.07025
2	0.000110	0.04437
3	0.000165	0.03773
4	0.000220	0.03510
5	0.000275	0.03382
6	0.000330	0.03310
7	0.000385	0.03326
8	0.000440	0.03237
9	0.000496	0.03218
10	0.000551	0.03203
11	0.000606	0.03192
12	0.000661	0.03184
13	0.000716	0.03178
14	0.000771	0.03172
15	0.000826	0.03169
16	0.000881	0.03166
17	0.000936	0.03162
18	0.000992	0.03160
19	0.001047	0.03159
20	0.001102	0.03157
21	0.001157	0.03155
22	0.001212	0.03154

The aforementioned data results in 3.15 %$<\left(\frac{\delta d,m}{d,m}\right)<$7%.

ENERGY EQUATION FOR ORIFICE

Applying Bernoulli's equation, between position 1 and 2 in Fig. 1,

$$\frac{P_1}{\gamma} + \frac{V_1^2}{2g} = \frac{P_2}{\gamma} + \frac{V_2^2}{2g} + h_{loss} \quad (6)$$

$$Q = C_d Q_{ideal} = C_d A_o \sqrt{\frac{2(P_1 - P_2)}{\rho(1-\beta^4)}} \quad (7)$$

Where β =d/D=0.4, is the diameter ratio of orifice and pipe. c_d is the orifice meter discharge coefficient,$(P_1 - P_2)$ pressure drop, ρ water density.

RESULTS AND DISCUSSION

Orifice coefficient of discharge was calculated from the measurements of orifice head difference and flow rate at different values of holdup (0, 15, 30, 45, 55, 60, 65%) for

stable and unstable oil-in-water emulsion flow. Figure (2) shows that orifice coefficient of discharge, C_d , for stable o/w emulsion with SDS emulsifier, is nearly constant for water, zero holdup, $\Phi = 0$. But, for $\Phi \succ 0$, C_d is slightly decrease with the increases Reynolds number. In addition, for the same Reynolds number C_d decreases as the holdup increases. This may be due to the increase of the viscosity as the holdup increase [11, 15, 16], the viscosity of emulsion increases as holdup increase, and this leads to decrease C_d as holdup increase. The results presented in Fig. 3 for stable emulsion with FAA emulsifier, show the same trend as explained before for the case of SDS emulsifier, Fig. (2). A comparison between the results presented in Figs. (2) and (3) shows that C_d for stable emulsion with FAA emulsifier is smaller than C_d for Stable emulsion with SDS emulsifier because the droplets for stable emulsion (FAA) is greater than (SDS) [11], and this means that the stable emulsion (SDS) viscosity is smaller than stable emulsion (FAA) viscosity [15, 16]. Due to the coarse droplets of unstable emulsion, the viscosity of unstable emulsion is smaller than the viscosity of stable emulsion at the same holdup. Thus, C_d for unstable emulsion, Fig.(4), is greater than stable one. Figure (5) Compares C_d for stable emulsion (SDS), stable emulsion (FAA), and unstable emulsion, as function in holdup. Empirical relations are derived to describe the orifice coefficient of discharge as function in holdup Φ .

$$C_{d\,(stableSDS)} = -2.02\phi^3 + 1.85\phi^2 - 0.66\phi + 0.7$$

R^2=0.98 (8)

$$C_{d\,(stableFAA)} = -3.15\phi^3 + 3.21\phi^2 - 1.19\phi + 0.7$$

R^2=0.98 (9)

$$C_{d\,(unstable)} = -0.136\phi^3 - 0.23\phi^2 - 0.06\phi + 0.7$$

R^2=0.99 (10)

R^2 is the square of the correlation between the experimental data values and the predicted fit values. R^2 can take any value between 0 and 1, with a value closer to 1 indicating a better fit. Thus, R^2 is a measure of how successful the fit is in explaining the variation of the experimental data. R^2 =0.98 for Eqs. (8-10).

The results of the pressure head difference before and after the orifice meter, $H = \frac{p_1 - p_2}{\rho G}$, are presented in Figures 6 , 7 and 8 for stable and unstable emulsions. These results show the same trend in all cases. In addition the trends of the experimental results are in agreement with the theoretical trend derived from Eq.7.

i.e $H \propto Q^2$ .The orifice head difference for stable emulsion with SDS emulsifier is shown in Fig. (6), where the head increases as holdup and flow rate increase. Figure (7) shows that for stable emulsion with FAA emulsifier, the head is greater than stable emulsion (SDS). For unstable emulsion, Fig.(8), the orifice head is less than stable one.

A photographic and subsequent image analysis technique, Fig. (9), was used to determine upstream and downstream droplet size distribution in unstable oil-in-water emulsion. Figure (10) shows the droplet size distribution and mean diameter upstream and downstream the orifice meter at holdup 30%. In Figure (10a) Re= 2434, and in Fig. (10b), Re=1785. Figures 10 a and b show that for certain droplet diameter in the smaller range (left of the figure) the results for upstream to the orifice meter of the number fraction of oil diameter is higher than the downstream ones. This situation is reversed for the case of bigger droplet. Meanwhile, it is clear from fig (10c) that the mean droplet diameter downstream to the orifice meter is smaller than upstream, due to breakup. Moreover, as the velocity increase, the energy loss increase, subsequently breakup increase, and thus the mean droplet diameter decreases. Figures 11 and 12 for holdup 45% (Re=1146, 846) and 55% (Re=504, 369) respectively show the same trends and consequently support the obtained results from figs.(10).

CONCLUSIONS

1-The orifice meter coefficient of discharge decreases and orifice head difference increases as the holdup increase.

2-For stable o/w emulsion, the type of surfactant has pronounced effect on coefficient of discharge and orifice pressure head difference.

3-The unstable o/w emulsion has greater value of coefficient of discharge and smaller orifice pressure head difference compared with stable emulsion.

4-The downstream mean droplet diameters are smaller than the upstream ones, due to breakup of drops passing through the orifice.

5- The drop breakup increases as the emulsion velocity increase.

6-As the holdup increased the mean droplet diameter increases, and this attributed to the drop coalescence process.

NOMENCLATURE

C_d	coefficient of discharge
H	head, m
P	pressure, Pa
Q	flow rate, m^3/s
T	temperature, ^oC
Φ	holdup
β	orifice diameter to pipe diameter ratio
γ	kinematics viscosity, c.stoke
μ	mixture viscosity, cp
ρ	mixture density, kg/m^3

List of Abbreviations

o/w	oil-in-water emulsions
SDS	sodium dodecyl sulfate
FAA	fatty acid and amine
ppi	pixels per inch

List of Chemical Symbols

$C_{18}H_{34}O_2$	oleic acid
C_3H_9N	trimethylamine
$CH_3(CH_2)_{11}OSO_3Na$	sodium dodecyl sulfate
$C_{16}\ H_{18}\ Cl\ N_3\ S\ 3H_2O$	methylene blue dye

REFERENCES

[1] S. Galinat, O. Masbernat, P. Guiraud, C. Dalmazzone, and C. Noik, "Drop Break-up in Turbulent Pipe Flow Downstream of a Restriction", *J.Chemical Engineering Science, Vol.60, pp. 6511-6528, 2005*.

[2] A. Buhidma, and R. Pal, " Flow measurement of two- phase oil –in-water emulsion using wedge meters and segmental orifice meters", *J.Chemical Engineering, Vol.63, pp 59-64, 1996.*

[3] T. S. Mayor, A. Pinto, and Campos, "An image analysis technique for the study of gas-liquid slug flow along vertical pipes-associated uncertainty", *Flow Measurement and Instrumentation, Article in Press, dol: 10.1016/ j.flowmeasinst. 2007.05.004, 2007.*

[4] J. S. Percy, and C. A. Sleicher, "Drop Breakup in the Flow of Immiscible Liquids Through an Orifice in a Pipe", *AIChE J., Vol. 29, No. 1, pp. 161-164, 1983*.

[5] H. Berthiaux, V. Mosorov, L. Tomczak, C. Gatumel, and J. F. Demeyre, "Principal Component Analysis for Characterising Homogeneity in Powder Mixing Using Image Processing Techniques", *J.Chemical Engineering and Processing, Vol.45, pp. 397-403, 2006*.

[6] N. Meijer, H. Abbes, and Wei G Hansen, "Particle Size Distribution and Dispersion of Oil-in-Water Emulsions: An Application of Light Microscopy", *American Laboratory, pp. 28-31, April, 2001.*

[7] J. Lovick, A. A. Mouza, S. V. Paras, G. J. Lye, and P. Angeli, "Droplet Size Distribution in Highly Concentrated Liquid-Liquid Dispersions Using a Light Back Scattering Method", *J. Chemical Technology and Biotechnology, Vol.80, pp. 545-552, 2005*.

[8] P. C. Mena, M. N. Pons, J. A. Teixeira, and F. A. Rocha, "Using Image analysis in the Study of Multiphase Gas Absorption", *Chemical Engineering Science, Vol.60, pp. 5144-5150, 2005.*

[9] M. F. Khalil, S. Z. Kassab, A. S. Ismail, and I. S. Elazab, " Friction Losses Of Oil-in-Water Emulsions Flow Through Pipes", *Cairo 10th International Conference on Energy and Environment (EE10), March 11-15, Luxor, Egypt, 2007a.*

[10] M. F. Khalil, S. Z. Kassab, A. S. Ismail, and I. S. Elazab, "Energy Losses of Stable and Unstable Oil-in-Water Emulsions Flow Through Pipe Fittings", *Cairo 10th International Conference on Energy and Environment (EE10), March 11-15, Luxor, Egypt, 2007b.*

[11] M. F. Khalil, S. Z. Kassab, A. S. Ismail, and I. S. Elazab, " Influence of Various Parameters on the Characteristics of Stable and Unstable Oil-in-Water Emulsion", *Proceedings of Eighth International Congress of Fluid Dynamics & Propulsion (ICFDP 8), Sharm El-Sheikh,Egypt, December 14-17, 2006.*

[12] M. J. O'Neil, A. Smith and P. E. Heckelman, "The Merck Index-An encyclopedia of chemicals, drugs, and biologicals", *Thirteenth edition, Merck & Co.,Inc, 2001*.

[13] O. D. Tyagi, and M. Yadav, " A Textbook of Synthetic Dyes", *Anmol Publications PVT LTD, New Delhi, INDIA, 2002*.

[14] D. A. Skoog, and D. M. West, "Fundamentals of Analytical Chemistry", *Holt, Rinehart and Winston , New York, 2001*.

[15] R. Pal, "Pipeline Flow of Unstable and Surfactant Stabilized Emulsions", *AIChE J., Vol. 39, No. 11, pp.1754-1764, 1993.*

[16] R. Pal, "Effects of Droplet Size and Droplet Size Distribution on the Rheology of Oil-in-Water Emulsions", *Chemical Engineering Department, Waterloo University, Internal Report,No. 1998.053,.1998*.

ANNEX A

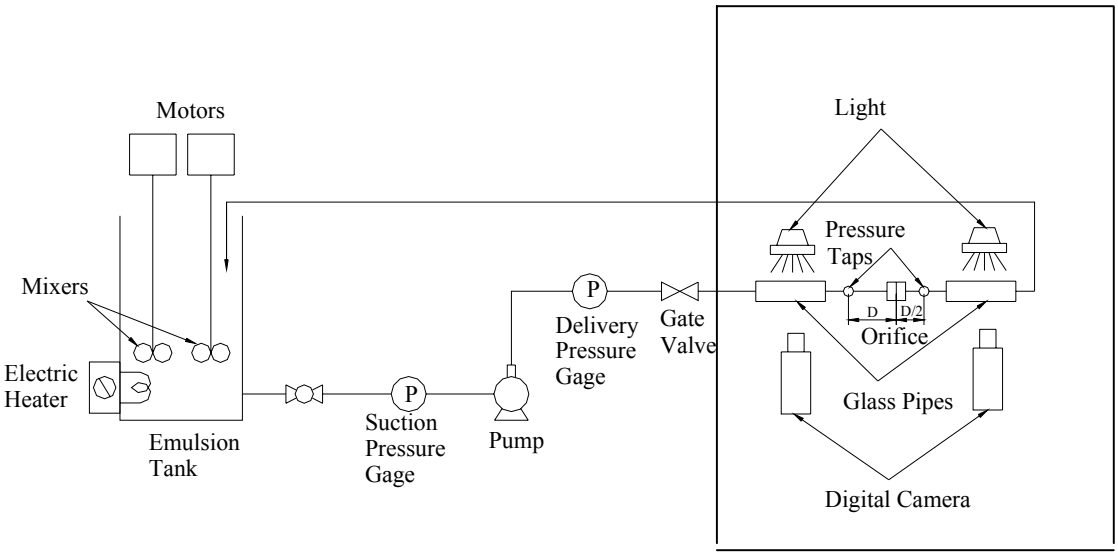

Fig. 1 The Test rig

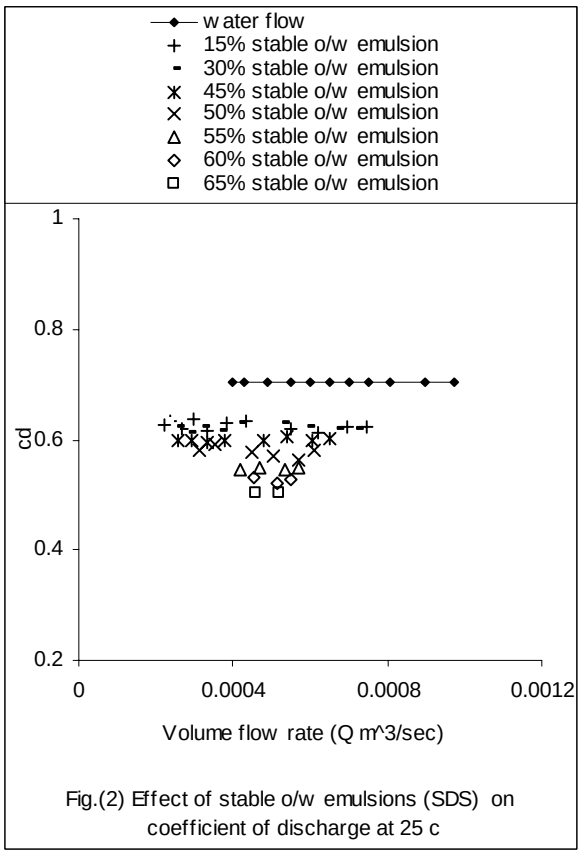

Fig.(2) Effect of stable o/w emulsions (SDS) on coefficient of discharge at 25 c

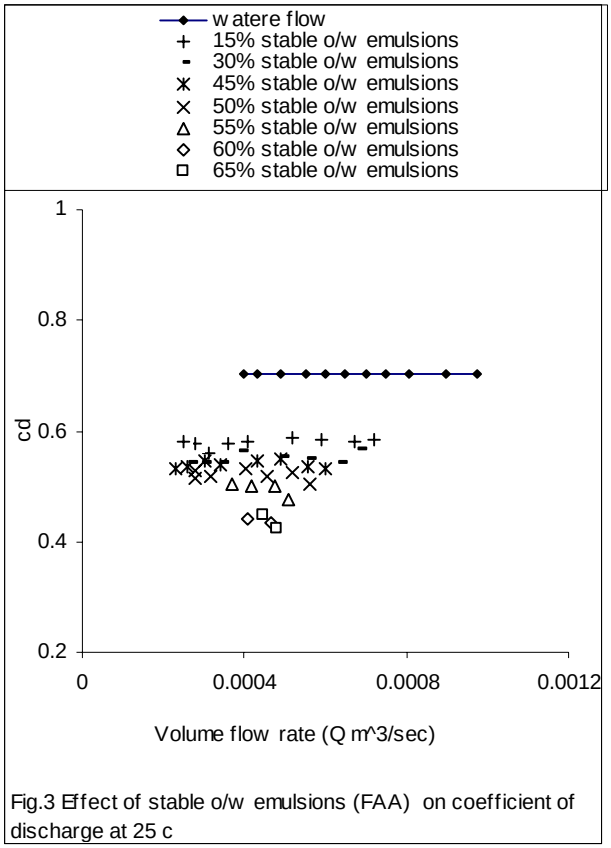

Fig.3 Effect of stable o/w emulsions (FAA) on coefficient of discharge at 25 c

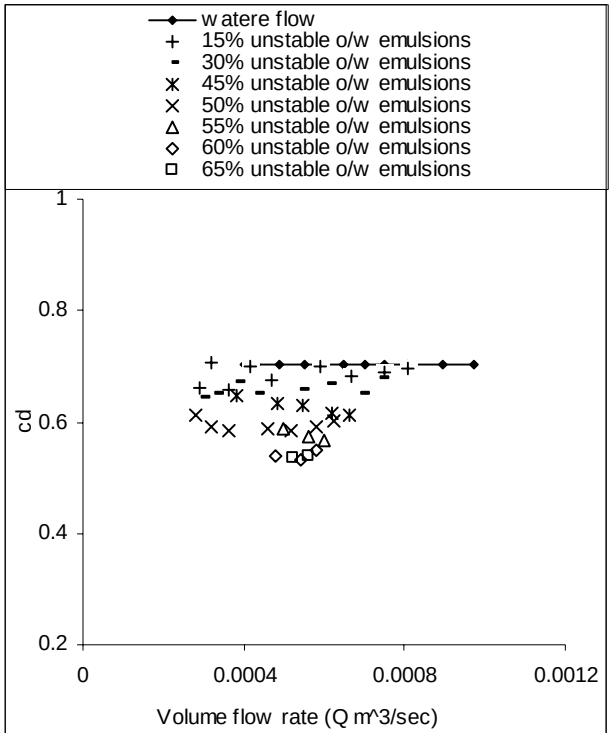

Fig.(4) Effect of unstable o/w emulsions on coefficient of discharge at 25 c

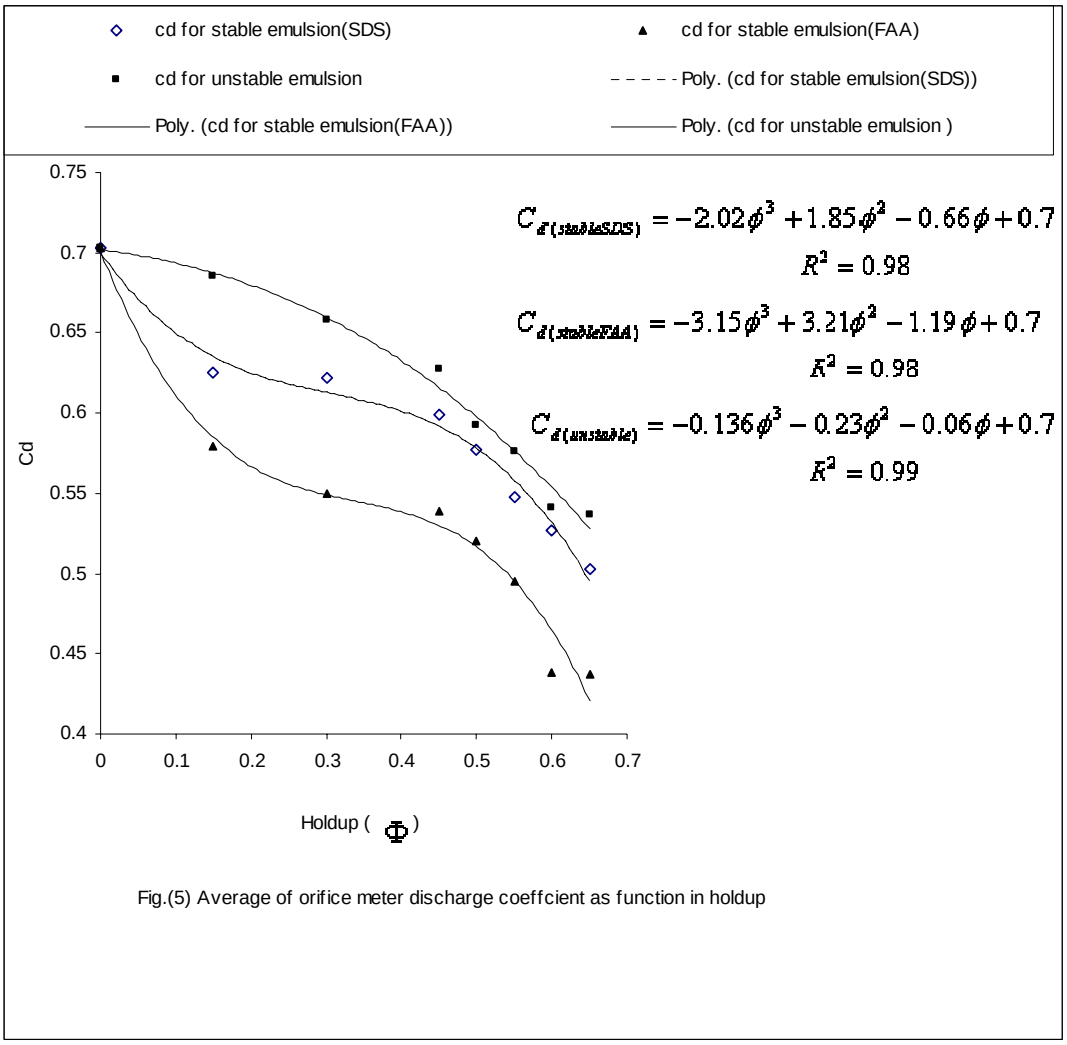

Fig.(5) Average of orifice meter discharge coeffcient as function in holdup

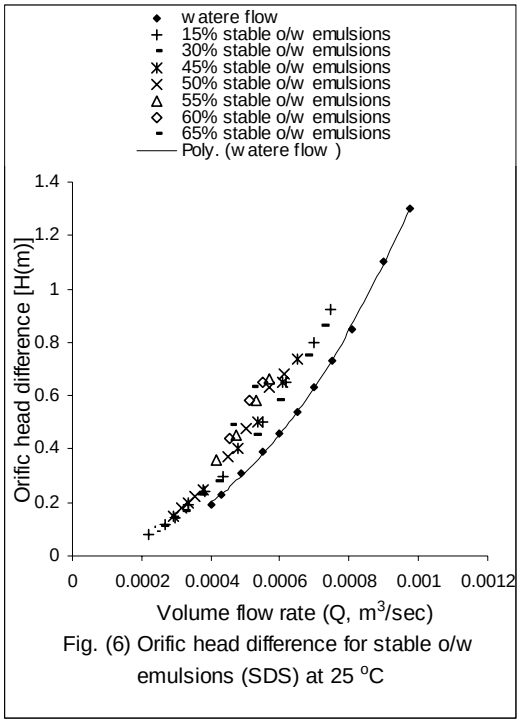

Fig. (6) Orific head difference for stable o/w emulsions (SDS) at 25 ^{o}C

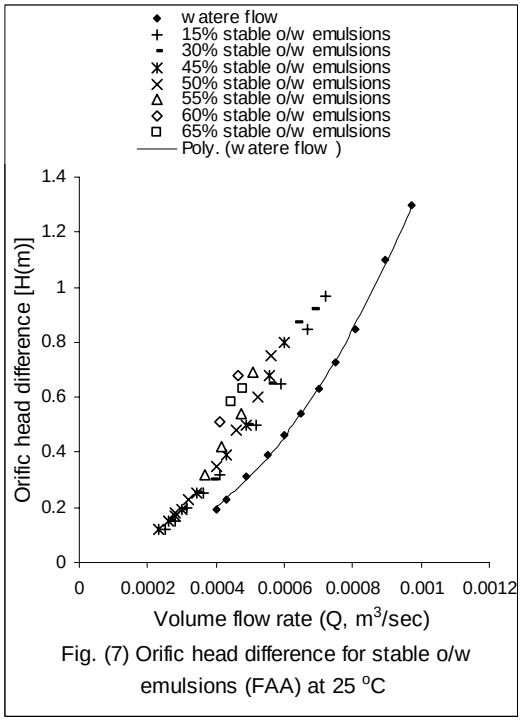

Fig. (7) Orific head difference for stable o/w emulsions (FAA) at 25 ^{o}C

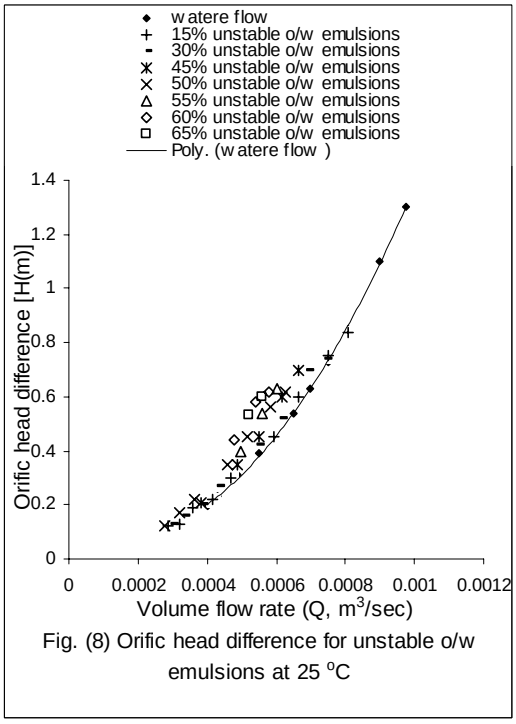

Fig. (8) Orific head difference for unstable o/w emulsions at 25 ^{o}C

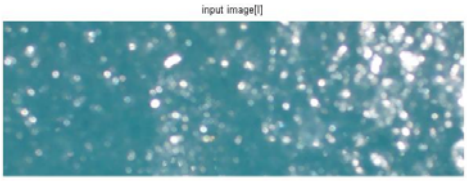

(1)Original

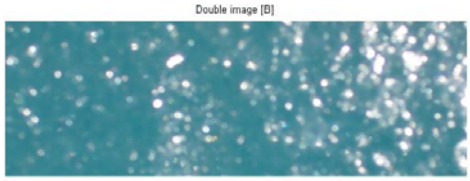

(2) Double

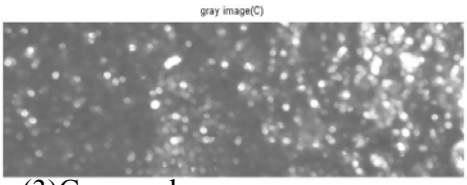

(3)Gray scale

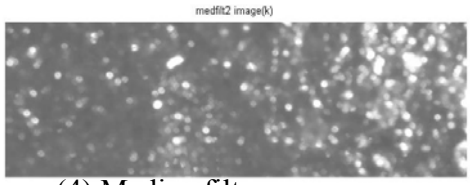

(4) Median filter

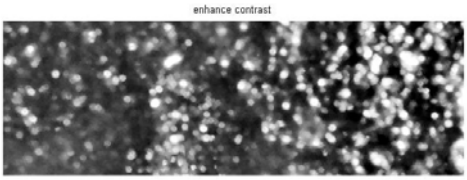

(5)Enhance contrast

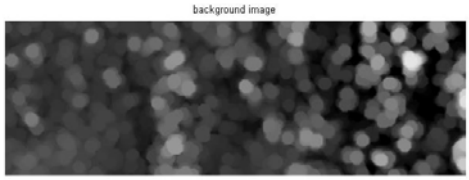

(6) background

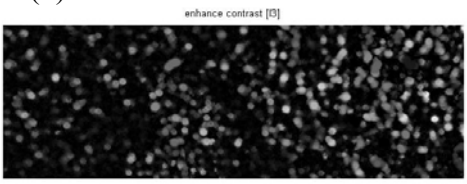

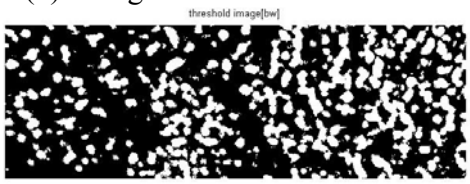

(7)After background subtraction and enhance contrast. (8)Threshold

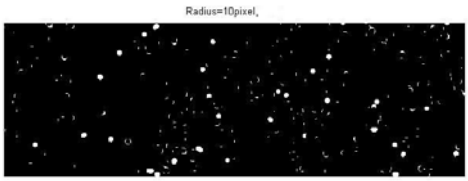

(9)Open at droplet radius 10 pixels

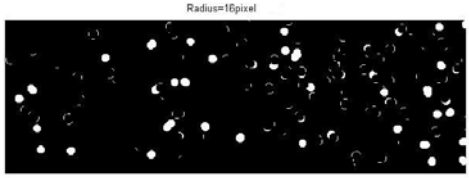

(10)Open at droplet radius 16 pixels

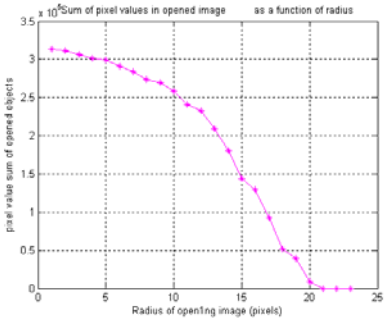

(11)Sum of pixel values

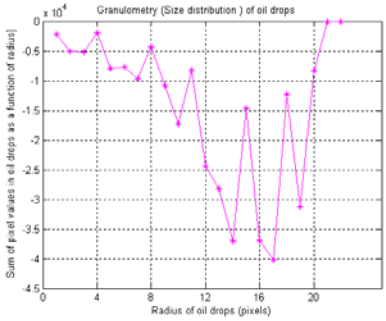

(12) Droplet size distribution in pixels

Fig.(9) Image analysis procedure upstream the orifice meter, 30% holdup, Re=1785.

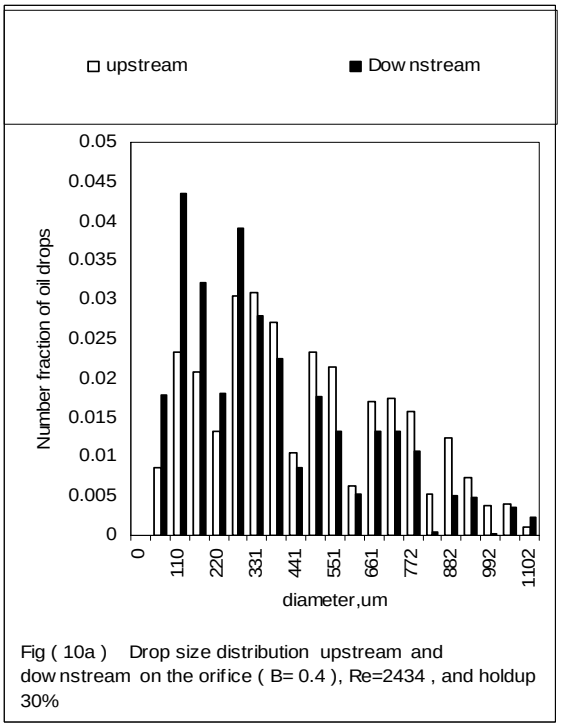

Fig (10a) Drop size distribution upstream and dow nstream on the orifice (B= 0.4), Re=2434 , and holdup 30%

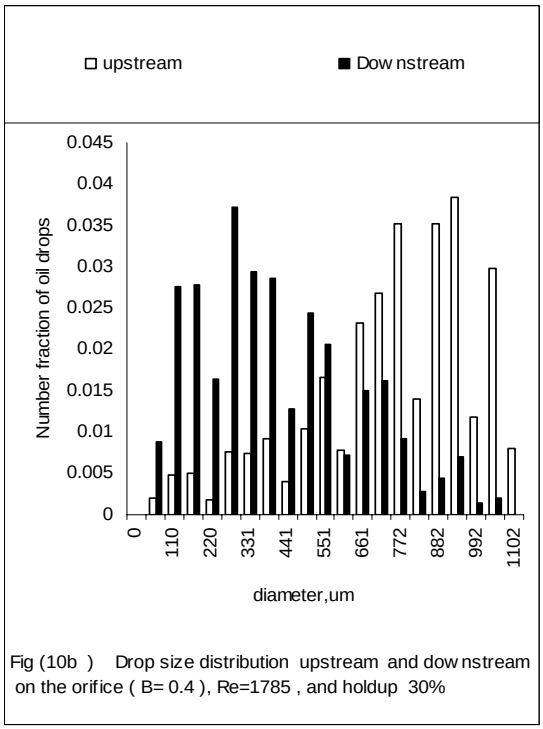

Fig (10b) Drop size distribution upstream and dow nstream on the orifice (B= 0.4), Re=1785 , and holdup 30%

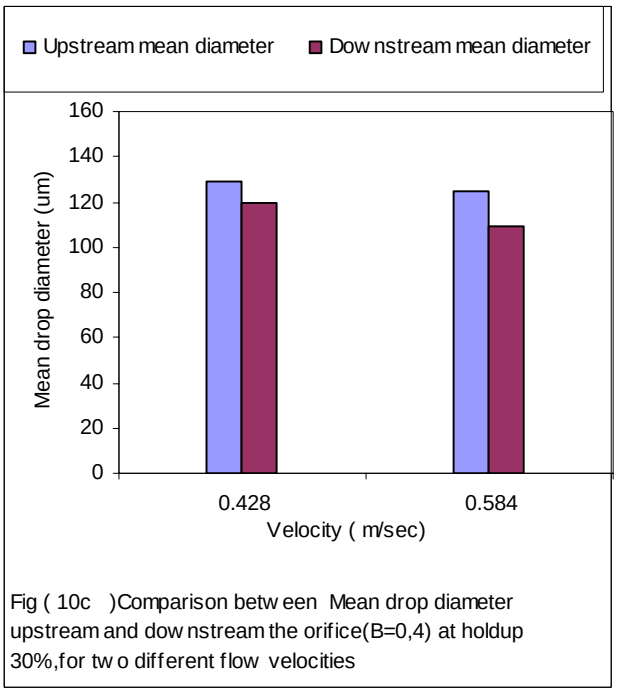

Fig (10c)Comparison betw een Mean drop diameter upstream and dow nstream the orifice(B=0,4) at holdup 30%,for tw o different flow velocities

Fig. (10) Effect of Reynolds number on droplet size distribution upstream and downstream the orifice at holdup 30%

a) Re=2434 b) Re=1785 c) Mean droplet diameter

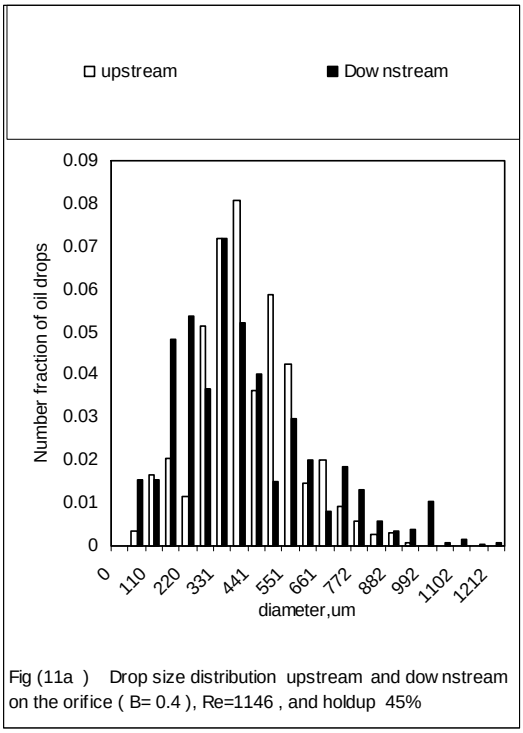

Fig (11a) Drop size distribution upstream and dow nstream on the orifice (B= 0.4), Re=1146 , and holdup 45%

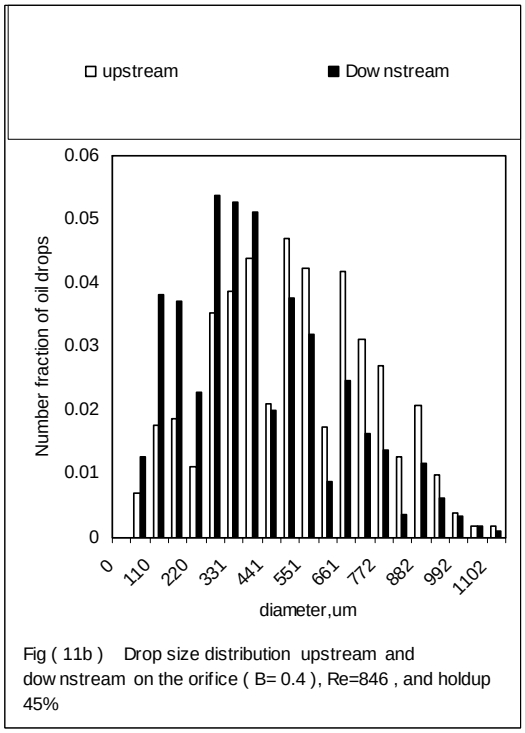

Fig (11b) Drop size distribution upstream and dow nstream on the orifice (B= 0.4), Re=846 , and holdup 45%

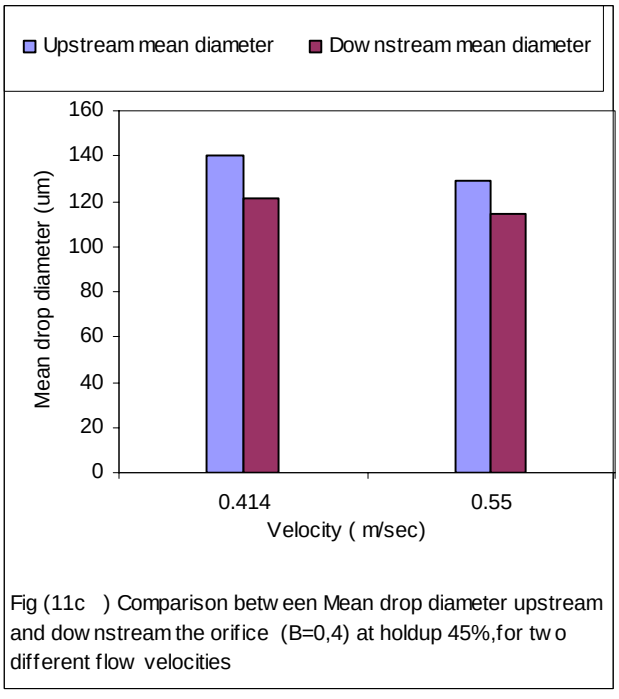

Fig (11c) Comparison betw een Mean drop diameter upstream and dow nstream the orifice (B=0,4) at holdup 45%,for tw o different flow velocities

Fig. (11) Effect of Reynolds number on droplet size distribution upstream and downstream the orifice at holdup 45%.

a) Re=1146 b) Re=846 c) Mean droplet diameter

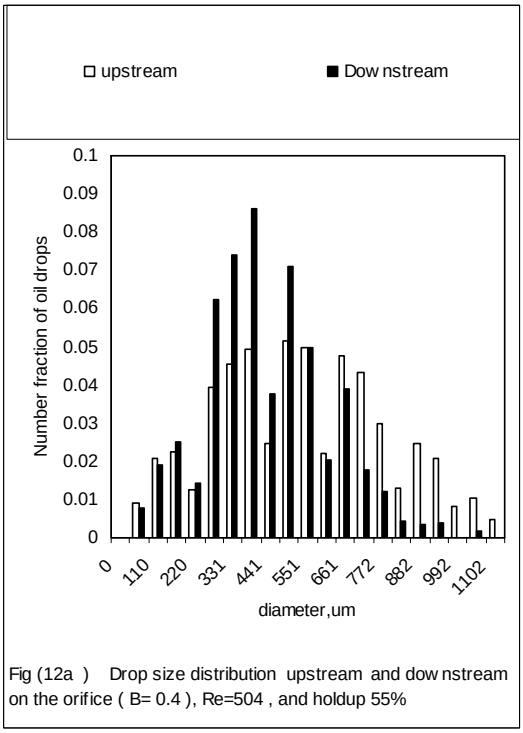

Fig (12a) Drop size distribution upstream and dow nstream on the orifice (B= 0.4), Re=504 , and holdup 55%

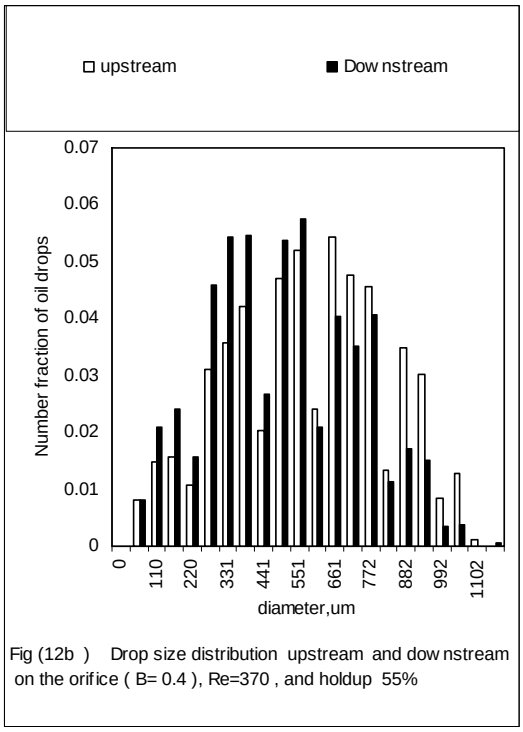

Fig (12b) Drop size distribution upstream and dow nstream on the orifice (B= 0.4), Re=370 , and holdup 55%

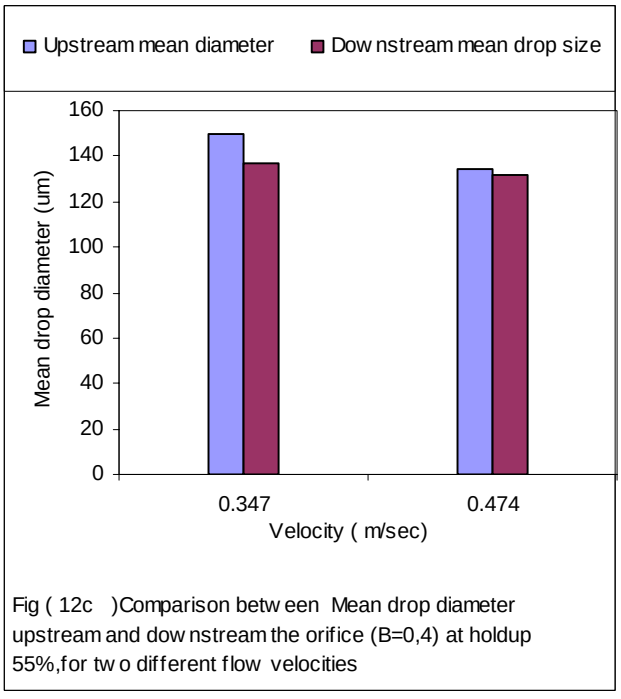

Fig (12c)Comparison betw een Mean drop diameter upstream and dow nstream the orifice (B=0,4) at holdup 55%,for tw o different flow velocities

Fig. (12) Effect of Reynolds number on droplet size distribution upstream and downstream the orifice at holdup 55%.

a) Re=504 b) Re=369 c) Mean drop diameter